ATLAS NOTE

ATL-PHYS-PUB-2014-021

2nd November 2014

ATLAS Pythia 8 tunes to 7 TeV data

The ATLAS Collaboration

Abstract

We present tunes of the PYTHIA 8 Monte Carlo event generator's parton shower and multiple parton interaction parameters to a range of data observables from ATLAS Run 1. Four new tunes have been constructed, corresponding to the four leading-order parton density functions, CTEQ6L1, MSTW2008LO, NNPDF23LO, and HERAPDF15LO, each simultaneously tuning ten generator parameters. A set of systematic variations is provided for the NNPDF tune, based on the eigentune method. These tunes improve the modeling of observables that can be described by leading-order + parton shower simulation, and are primarily intended for use in situations where next-to-leading-order and/or multileg parton-showered simulations are unavailable or impractical.

1 Introduction

Several Monte Carlo (MC) event generators use parton shower, hadronisation, and multiple interaction models to enhance fixed-order partonic matrix element events and produce simulated events as similar as possible to real collider data. These models are typically either approximations to high-multiplicity perturbative QCD calculations, or phenomenological attempts to address non-perturbative physics which is not understood from first principles; accordingly each model presents several free parameters which must be optimised to produce a reasonable description of measured observables. This optimisation process is known as tuning, and the resulting parameter sets are referred to as MC generator tunes.

ATLAS has previously used early LHC Run 1 data to tune the multiparton interaction (MPI) parameters in Pythia 8 [1], resulting in the extensively used AU2 tune series (with various parton density functions (PDFs)) for simulation of underlying event (UE) in hard interaction events, and the A2 tune for minimum bias (MB) / pile-up event simulation [2]. Previous ATLAS studies have also tuned a subset of Pythia 8 and Powheg +Pythia 8 model parameters to specifically improve the modelling of the Z-boson transverse momentum (p_{T}) distribution [3].

In this note, standalone Pythia 8 tunes at $\sqrt{s}$ = 7 TeV for high p_{T} events are presented, in which tuning of MPI and initial & final state radiation (ISR,FSR) parameters has been performed in a single step, using most of the available Run 1 data. Separate tunes have been performed for four leading-order (LO) parton density functions – CTEQ6L1, MSTW2008LO, NNPDF23LO, and HERAPDF15LO – producing a set of four tunes which we designate as the "A14" (ATLAS 2014) tune series. Additionally, systematic variations on the NNPDF23LO tune variant have been made, by finding variations along the principle directions of the covariance matrix at the tune minimum (the "eigentune" method); these variations provide good coverage of the experimental and modelling uncertainties implicit in the tuning.

The data used in this tuning includes ATLAS observables sensitive to:

- underlying event (evolution of transverse activity with leading track & calorimeter jets [4, 5])
- jet structure (track jet properties [6], jet masses & other substructure variables [9], and jet shapes in inclusive jet and $t\bar{t}$ events [7, 8])
- observables sensitive to additional jet emissions above the lowest-order process (dijet azimuthal decorrelation [10], $t\bar{t}$ gap fraction [11], the 3/2 jet ratio [12], and Z-boson p_{T} [13, 14]).

In the roughest approximation, these three classes of observables are determined respectively by modelling of multiple partonic interactions, of final state parton showering, and of initial state showering. And indeed these are the dominant features seen in tuning. However, such a clean factorisation is not the whole story, and in practice shower modelling can affect underlying event observables, the final state shower can affect additional jet emissions, etc.

Care has been taken to achieve a single tune series for stand-alone Pythia 8 which can describe the wide variety of event topologies from inclusive Z-boson to $t\bar{t}$ production, by avoiding phase space regions where multijet hard processes are essential and by choosing appropriate process-specific schemes for the initial-state parton shower high-p_{T} emission threshold. Additional tunes are in preparation for use with higher-order matrix elements.

As for the previous studies, the Rivet analysis toolkit [15] and the Professor MC tuning system [16] were used, at versions 2.1.2 and 1.4.beta respectively. The PYTHIA 8 version used was 8.186, with the PDFs taken from LHAPDF version 6.1.3 [17].

2 Central tunes

2.1 Tuning setup

Previously ATLAS has optimised the shower and MPI parameters for PYTHIA 6 generator iteratively in separate tuning stages [18, 19, 20]. However, as physics studies at the LHC have shown, it is difficult to isolate observables sensitive only to the MPI due to significant contributions from hard process radiation to the standard underlying event observables [5, 21]. It was therefore decided to tune the MPI parameters simultaneously with those governing shower and matrix element (ME) couplings, parton shower damping and matching, and colour reconnection. This avoids the need for separate tune stages and resulting complexities, and properly accounts for the mixture of MPI and QCD radiation effects on the observables.

A detailed description of the tuned parameters is beyond the scope of this note, and the reader is referred to the PYTHIA 8 online documentation. They divide roughly into the hard process strong coupling `SigmaProcess:alphaSvalue`, initial and final state parton shower scales and couplings (`SpaceShower:*` and `TimeShower:*` parameters), and the strong coupling and regularisation of multiple partonic interactions (`MultipartonInteractions:*` parameters). Two "beam-remnant" parameters are also tuned: the `primordialKThard` which generates a narrow Gaussian intrinsic transverse momentum for the hard process incoming partons, and the strength of the phenomenological colour-string reconnection mechanism. The tuned parameters are listed in Table 1, with a very brief definition, along with their sampling range used for the current tune.

Five hundred parameter points were randomly sampled from the hypercube of these parameter ranges. For each of these points, 1 million events were generated for each of the dijet, $t\bar{t}$, and single Z-boson hard processes, the jets process being run with high-p_{T}-enhanced weighted matrix element sampling to cover large and small leading jet scales within a single MC run. The remaining parameters were left unchanged from the Monash tune [22]. The Monash configuration uses an exponential overlap function (`MultipartonInteractions:bProfile = 3`, exponent `MultipartonInteractions:expPow`) as opposed to the double Gaussian matter profile of the AU2 tunes (with `MultipartonInteractions:bProfile = 4`). The PYTHIA 8 MPI modelling also includes a power law dependence of the MPI screening scale, controlled by the `MultipartonInteractions:ecmPow` parameter – this was not included in the A14 tuning since earlier tune iterations agreed with the Monash value of 0.215. Also `SpaceShower:rapidityOrder = on` was used, motivated by previous ATLAS tunes.

Table 2 shows the observables used in the A14 tuning. Each bin of each observable was parameterised as a 10-dimensional 3rd order polynomial, based on the 500 sampled tune points in the parameter hypercube. These parameterisations were then used to calculate a χ^2 with respect to the reference data, which was numerically minimised in the parameter space to find the best tune point. Weight factors were used in the χ^2 and degree of freedom, N_{df}, calculation to place increased emphasis on certain observables; these weights are also listed in Table 2.

The strategy was to tune only to observables which may be modelled by parton-showered lowest-order

Parameter	Definition	Sampling range
`SigmaProcess:alphaSvalue`	The α_S value at scale $Q^2 = M_Z^2$	0.12 – 0.15
`SpaceShower:pT0Ref`	ISR p_{T} cutoff	0.75 – 2.5
`SpaceShower:pTmaxFudge`	Mult. factor on max ISR evolution scale	0.5 – 1.5
`SpaceShower:pTdampFudge`	Factorisation/renorm scale damping	1.0 – 1.5
`SpaceShower:alphaSvalue`	ISR α_S	0.10 – 0.15
`TimeShower:alphaSvalue`	FSR α_S	0.10 – 0.15
`BeamRemnants:primordialKThard`	Hard interaction primordial $k_\perp$	1.5 – 2.0
`MultipartonInteractions:pT0Ref`	MPI p_{T} cutoff	1.5 – 3.0
`MultipartonInteractions:alphaSvalue`	MPI α_S	0.10 – 0.15
`BeamRemnants:reconnectRange`	CR strength	1.0 – 10.0

Table 1: Tuning parameters, their definition and tuning range

matrix elements, with the parton shower at most being relied on to mimic the emission of a single additional hard jet. The observables affected by emission of several extra jets require multi-leg generators for a robust description, and relying on the parton shower to produce sufficient hard emissions could drive the model to an unresolvable tension between observables. Observable regions very sensitive to multiple extra emissions were hence excluded from this tuning, for example the transverse momentum of the Z-boson, $p_{\mathrm{T}}^{\mathrm{Z}}$ above 50 GeV, and dijet azimuthal decorrelations far away from the leading-order back-to-back configuration.

These region exclusions and the tuning weights (and final sampling ranges) were arrived at by using observable sensitivities to find data tensions, and by iteration. Weight assignment was performed by eye, generally following the principles that important features measured in a small number of distributions (for example the 3/2 jet multiplicity ratio) would receive an increased weight to balance them against features for which many histograms were available. A more qualitative judgement was made in assigning reduced weights to observables considered less important for the BSM-dominated use-cases of these tunes, or where the model appeared to be incapable of fully describing them, for example the reduction of weight for the $p_{\mathrm{T}}^{\mathrm{Z}}$ and the high-$|y|$ $t\bar{t}$ jet gap fractions.

The same weights have been used for several different PDFs to produce a set of equivalent tunes.

2.2 Tunes

Tunes have been made for four different leading order PDFs: the central members of the CTEQ6L1 [23], MSTW2008LO [24], NNPDF23LO [25] and HERAPDF15LO [26] PDF sets. Table 3 shows the tune parameters for all the tunes corresponding to different PDFs.

In Figs. 1–6, the performance of the A14 tunes corresponding for the four different PDFs can be seen for $t\bar{t}$, Z-boson and jet observables.

Observable	Fit range	Weight
Track jet properties [6]		
Charged jet multiplicity (50 distributions)		10.0
Charged jet z (50 distributions)		10.0
Charged jet $p_{\mathrm{T}}^{\mathrm{rel}}$ (50 distributions)		10.0
Charged jet $\rho_{\mathrm{ch}}(r)$ (50 distributions)		10.0
Jet shapes [7]		
Jet shape ρ (59 distributions)		10.0
Dijet decorr [10]		
Decorrelation $\Delta\phi$ (9 distributions)	$\Delta\phi > 0.75$	20.0
Multijets [12]		
3-to-2 jet ratios (8 distributions)		100.0
$\boldsymbol{p_{\mathrm{T}}^{\mathrm{Z}}}$ [13, 14]		
Z-boson p_{T} (20 distributions)	$p_{\mathrm{T}}^{\mathrm{Z}} < 50$ GeV	10.0
Substructure [9]		
Jet mass, $\sqrt{d_{12}}$, $\sqrt{d_{23}}$, τ_{21}, τ_{23} (36 distributions)		5.0
$\boldsymbol{t\bar{t}}$ **gap** [11]		
Gap fraction vs Q_0, Q_{sum} for $\lvert y\rvert < 0.8$		100.0
Gap fraction vs Q_0, Q_{sum} for $0.8 < \lvert y\rvert < 1.5$		80.0
Gap fraction vs Q_0, Q_{sum} for $1.5 < \lvert y\rvert < 2.1$		40.0
Gap fraction vs Q_0, Q_{sum} for $\lvert y\rvert < 2.1$		10.0
$\boldsymbol{t\bar{t}}$ **jet shapes** [8]		
Jet shapes $\rho(r)$, $\psi(r)$ (20 distributions)		5.0
Track-jet UE [4]		
Transverse region N_{ch} profiles (5 distributions)		10.0
Transverse region mean p_{T} profiles for $R = 0.2, 0.4, 0.6$ (3 distributions)		10.0
Jet UE [5]		
Transverse, trans-max, trans-min sum p_{T} incl. profiles (3 distributions)		20.0
Transverse, trans-max, trans-min N_{ch} incl. profiles (3 distributions)		20.0
Transverse sum E_{T} incl. profiles (2 distributions)		20.0
Transverse sum E_{T}/sum p_{T} ratio incl., excl. profiles (2 distributions)		5.0
Transverse mean p_{T} incl. profiles (2 distributions)		10.0
Transverse, trans-max, trans-min sum p_{T} incl. distributions (15 distributions)		1.0
Transverse, trans-max, trans-min sum N_{ch} incl. distributions (15 distributions)		1.0

Table 2: Observable–weight combinations used for the tuning. Where the fit has been made to a restricted range, the fit range for that weight is shown in the "Fit range" column.

Param	CTEQ	MSTW	NNPDF	HERA
`SigmaProcess:alphaSvalue`	0.144	0.140	0.140	0.141
`SpaceShower:pT0Ref`	1.30	1.62	1.56	1.61
`SpaceShower:pTmaxFudge`	0.95	0.92	0.91	0.95
`SpaceShower:pTdampFudge`	1.21	1.14	1.05	1.10
`SpaceShower:alphaSvalue`	0.125	0.129	0.127	0.128
`TimeShower:alphaSvalue`	0.126	0.129	0.127	0.130
`BeamRemnants:primordialKThard`	1.72	1.82	1.88	1.83
`MultipartonInteractions:pT0Ref`	1.98	2.22	2.09	2.14
`MultipartonInteractions:alphaSvalue`	0.118	0.127	0.126	0.123
`BeamRemnants:reconnectRange`	2.08	1.87	1.71	1.78

Table 3: Tuned parameters for the A14 set of tunes

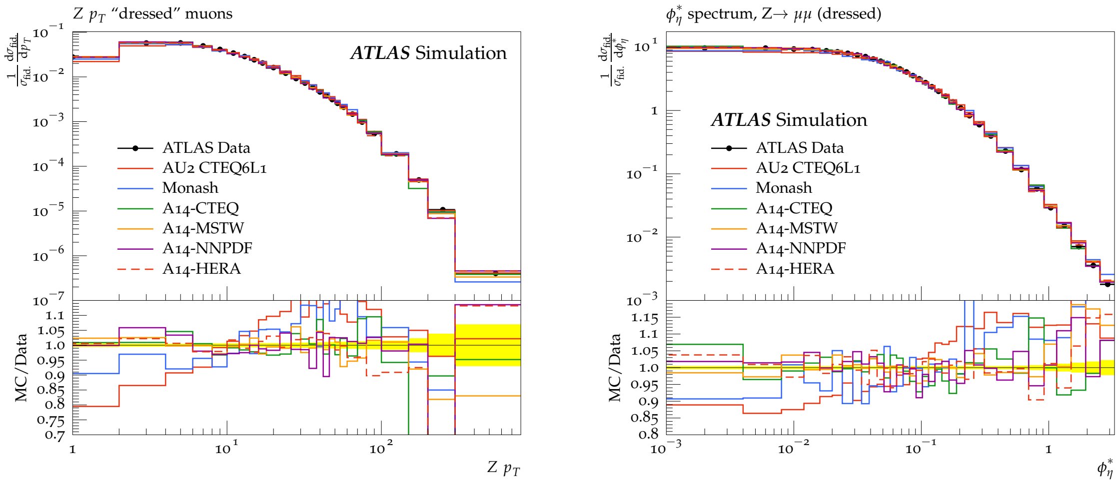

Figure 1: The A14, AU2 and Monash tune predictions compared with ATLAS p_T^Z [14] and Z-boson ϕ^* [27] distributions. The yellow shaded areas represent data uncertainty.

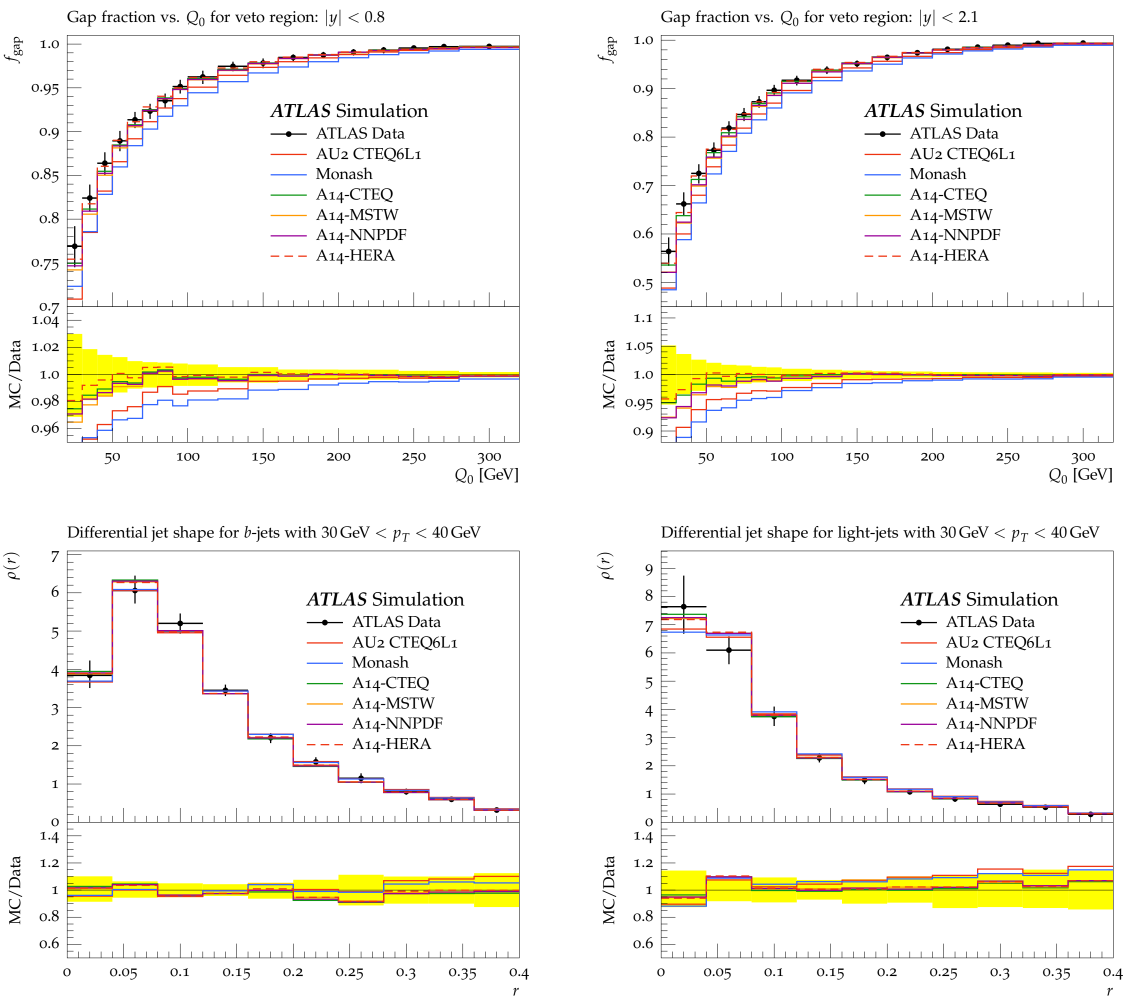

Figure 2: The A14, AU2 and Monash tune predictions compared with ATLAS $t\bar{t}$ gap [11] and $t\bar{t}$ jet shapes [8] distributions. The yellow shaded areas represent data uncertainty.

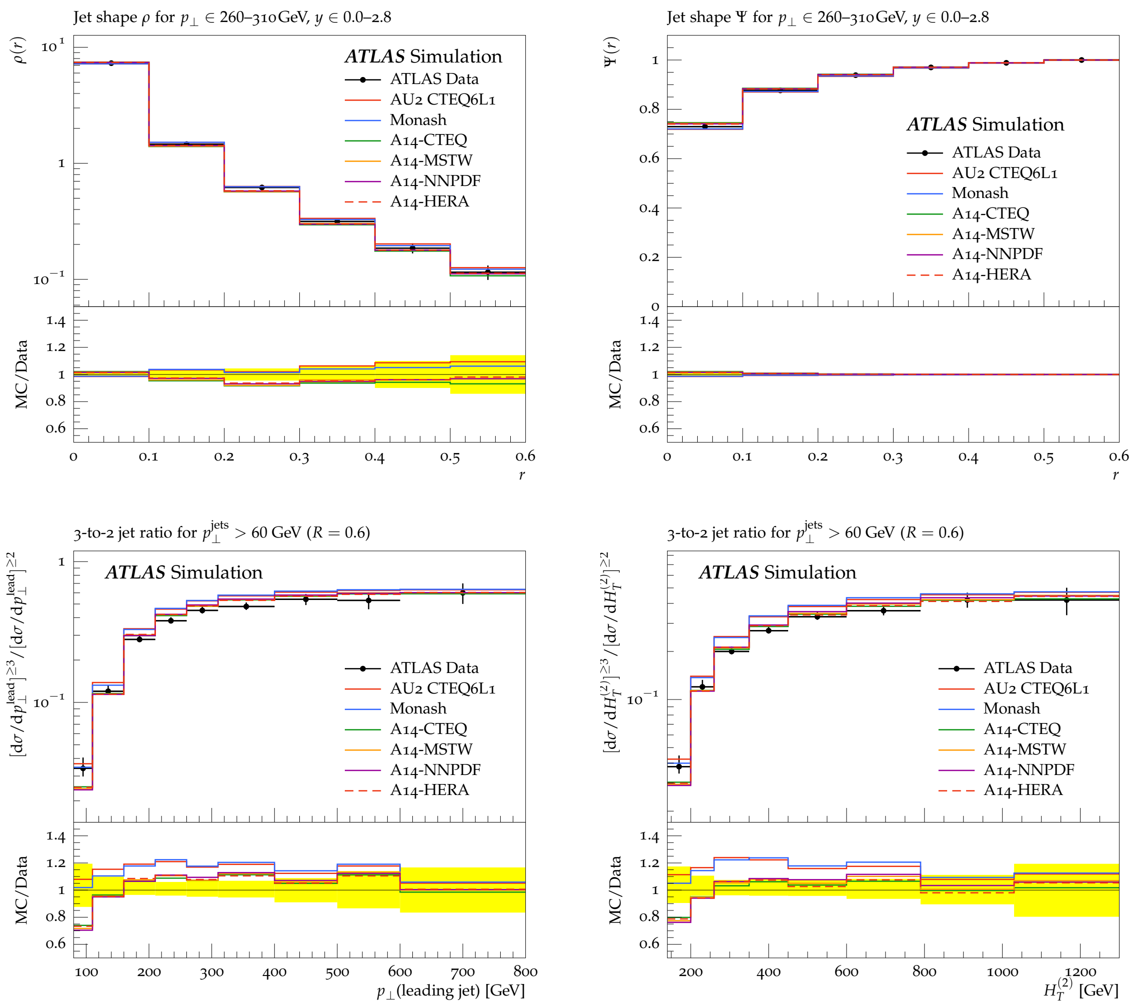

Figure 3: The A14, AU2 and Monash tune predictions compared with ATLAS jet shapes [7] and multijet 3-to-2 jet ratio [12] distributions. The yellow shaded areas represent data uncertainty.

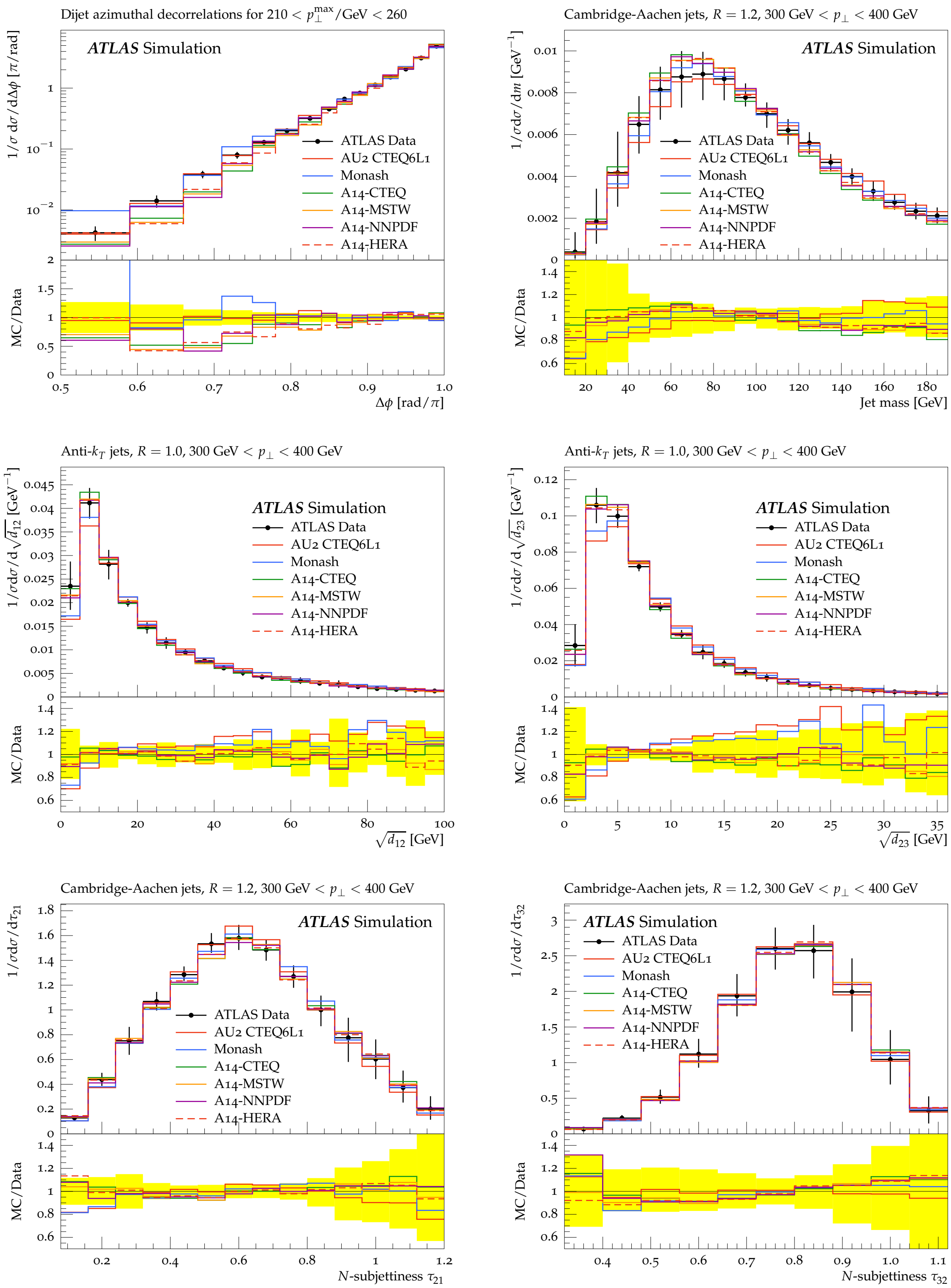

Figure 4: The A14, AU2 and Monash tune predictions compared with ATLAS dijet decorrelation [10] and jet substructure [9] observables. The yellow shaded areas represent data uncertainty.

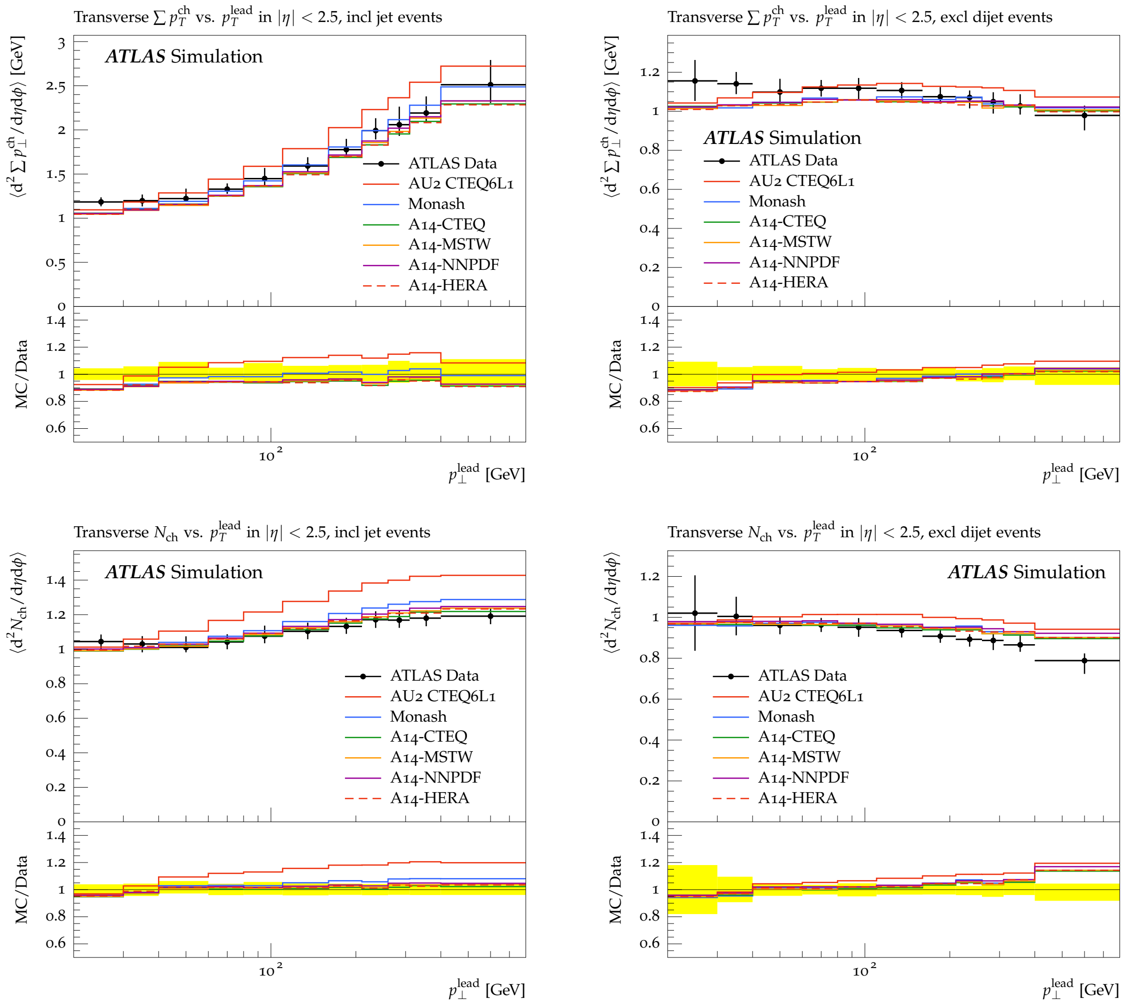

Figure 5: The A14, AU2 and Monash tune predictions compared with ATLAS jet underlying event [5] distributions. The yellow shaded areas represent data uncertainty.

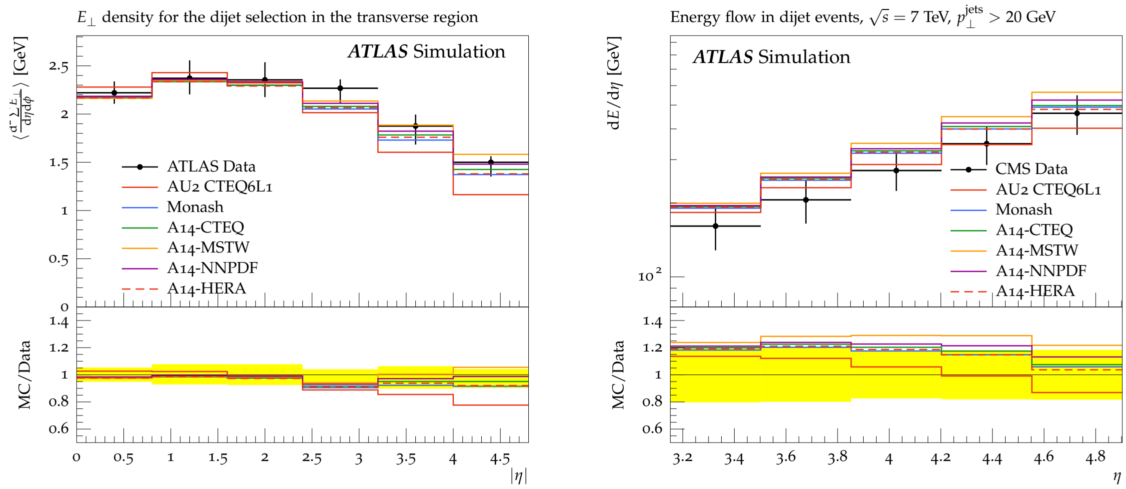

Figure 6: The A14, AU2 and Monash tune predictions compared with ATLAS transverse energy flow [28] and CMS forward energy flow [29] distributions. The yellow shaded areas represent data uncertainty.

2.2.1 Tune performance and features

For $t\bar{t}$ gap fraction and Z-boson observables, a significant improvement can be seen over AU2 and Monash tunes as a result of tuning the shower parameters. The jet shapes are equally good in both $t\bar{t}$ and dijet events, and a slight improvement can be seen in dijet decorrelation and substructure variables. The 3-to-2 ratios are significantly improved in the new tunes. For the underlying event and transverse energy flow observables, the new tunes significantly improve over AU2 and are similar to the performance of the Monash tune.

We note the following additional features:

- The tuned hard process QCD coupling, α_S, is similar for all four PDFs, and significantly higher than the default value of 0.1265. Since leading order cross-sections are not expected to be well-normalised, only shape information has been used in this tuning. In practice it is recommended that higher-order total cross-sections be used for normalisation when available, and scale variations should always be used, both at leading-order and beyond, to assess the normalisation model uncertainty.
- The ISR and FSR α_S values are again very similar between different PDFs and between ISR and FSR. They are significantly lower than the high default value of 0.137 and the Monash tune value of 0.1365. This may indicate slight tension between the LHC jet structure data and the LEP differential jet rates used to tune the Monash FSR shower.
- A damped shower was used for the $t\bar{t}$ process to include some emissions above the factorization scale. This significantly improved the modelling of the $t\bar{t}$ gap fraction with respect to the bare wimpy or power shower, by allowing some emissions above the top mass and hence re-shaping the MC gap survival function. This improved performance is shown in Fig. 2. This mode was enabled by setting `SpaceShower:pTmaxMatch = 2`, `SpaceShower:pTdampMatch = 1` and tuning `SpaceShower:pTdampFudge`. For Z-boson processes, the power shower (`SpaceShower:pTmaxMatch = 2`) was used, consistent with the Pythia 8 authors' recommendations.
- Using the damped shower for the $t\bar{t}$ process reduced tension with the p_{T}^{Z} and 3-to-2 jet multiplicity ratio distributions in Fig. 1 and Fig. 3, permitting a consistent tune setup for all three process types with good data description in all processes. This was also helped by restricting $p_{\mathrm{T}}^{Z} < 50$ GeV. Without these restrictions and model variations, Pythia 8 was found to be unable to simultaneously describe these different ISR-driven observables.
- The good modelling of 3-to-2 jet ratio shows that the shower is mimicking the 3rd ME leg, describing the ratio better than the Monash and AU2 tunes for most values of jet $p_{\mathrm{T}}^{\mathrm{lead}}$ and $H_T^{(2)}$. This comes at the cost of a less good description of σ_3/σ_2 in relatively soft events, e.g. $p_{\mathrm{T}}^{\mathrm{lead}} < 100$ GeV. We consider this an appropriate trade-off, given that multijet matrix elements are available for pure QCD jet production and the target use-case of these tunes is BSM simulation where higher-order shower-matched matrix elements are unavailable.
- Jet shapes are well modelled by all the tunes both in dijet and $t\bar{t}$ events.
- In Fig. 4, dijet decorrelation, jet gap and jet substructure observables are shown. Dijet decorrelation is modelled well in near-back-to-back topologies. Jet substructure description is also affected

by FSR, and is all within the uncertainty bands, with some distinction between the A14 and AU2/Monash tune characteristics.

- The MPI parameters are sensitive to the PDF used, as seen in previous studies.
- Generally good agreement is observed for jet UE distributions, as in Fig. 5. There is a slight undershoot at the first bins of exclusive dijet distribution, which the model could not be tuned to describe. Other track-jet, leading-track, leading-cluster UE modelling also consistently good with these tunes.
- In Fig. 6, the ATLAS dijet transverse energy, E_T, distribution is well modelled by the tunes. There is some PDF dependence, with HERAPDF predicting lower activity, and MSTW2008LO predicting slightly higher activity. There is a mild offset of these tunes to ATLAS data when compared to the forward energy sum distribution from CMS [29], at the level of $\sim 1\sigma$, given that the uncertainties are systematics-dominated and likely correlated between the observable bins.
- The colour reconnection range is quite consistent across the four tunes/PDFs, indicating a fairly well defined value of between 1.7 and 2.1. This gives slightly stronger colour reconnection than in the default 4C tune (with a value of 1.5), and is consistent with the Monash tune value of 1.8.

3 Systematic variation tunes

Systematic variations on the parameters of the A14-NNPDF tune have been performed using the eigentunes approach encoded in the Professor toolkit. The NNPDF2.3LO PDF variant was chosen as it is the most recent LO PDF fit, and contains an “error set” for evaluating PDF uncertainties; it is hence a good candidate for large-scale MC sample production. This method diagonalises the χ^2 covariance matrix around the best fit point, and uses excursions along the principle directions in parameter space to build a set of $2 \times N_{\text{param}}$ variations with fixed $\Delta\chi^2$. For this tune $\chi^2 = 3.44 \times 10^5$ for $N_{\text{df}} = 80315$, giving a χ^2/N_{df} of 4.29. This goodness of fit variable cannot be interpreted directly as obeying χ^2 distribution statistics – among other limitations, it does not account for correlations in systematic uncertainties between observables and bins – and hence the $\Delta\chi^2$ was chosen manually to provide reasonable coverage of the experimental data errors across the set of observables. Using a standard heuristic approach with $\Delta\chi^2 = N_{\text{df}}$ was found to give conservative coverage of the experimental errors, and hence a modified $\Delta\chi^2 = N_{\text{df}}/2 = 40157$ choice was made, giving appropriate levels of observable variation.

As this combined FSR, ISR and MPI tune has ten parameters, an eigentunes approach strictly produce 20 independent variation tunes, the full set of which must be used to cover the uncertainties. This is too unwieldy for regular use, so we have by inspection reduced it to a subset of tune variations which together provide maximal coverage of the observables: one pair mainly for underlying event effects, one pair mainly for jet structure effects, and three pairs for different aspects of extra jet production. The variation tune parameters are listed in Table 4 as groups VAR1–VAR3{a,b,c}, in which parameters which changed by less than 1% from their best fit value have been elided. Fig. 7 shows the spread of these eigentunes for a few selected distributions.

The latter group of three jet-production variations unfortunately could not be reduced to a single pair of tune variations, and whether it is appropriate to use one or all of these variations depends on the physics to be studied. We do not prescribe an approach, and in general all five variation pairs should be used in

Param	+ variation	− variation
VAR1: MPI+CR (UE activity and incl jet shapes)		
`BeamRemnants:reconnectRange`	1.73	1.69
`MultipartonInteractions:alphaSvalue`	0.131	0.121
VAR2: ISR/FSR (jet shapes and substructure)		
`SpaceShower:pT0Ref`	1.60	1.50
`SpaceShower:pTdampFudge`	1.04	1.08
`TimeShower:alphaSvalue`	0.139	0.111
VAR3a: ISR/FSR ($t\bar{t}$ gap)		
`MultipartonInteractions:alphaSvalue`	0.125	0.127
`SpaceShower:pT0Ref`	1.67	1.51
`SpaceShower:pTdampFudge`	1.36	0.93
`SpaceShower:pTmaxFudge`	0.98	0.88
`TimeShower:alphaSvalue`	0.136	0.124
VAR3b: ISR/FSR (jet 3/2 ratio)		
`SpaceShower:alphaSvalue`	0.129	0.126
`SpaceShower:pTdampFudge`	1.04	1.07
`SpaceShower:pTmaxFudge`	1.00	0.83
`TimeShower:alphaSvalue`	0.114	0.138
VAR3c: ISR ($t\bar{t}$ gap, dijet decorrelation and Z-boson p_{T})		
`SpaceShower:alphaSvalue`	0.140	0.115

Table 4: Parameters for five pairs of eigentunes, with distributions most sensitive to that variation indicated.

quadrature to get full coverage of the tune uncertainties. However, depending on analysis circumstances it may be possible to adequately cover the modelling uncertainties with three pairs of variations, roughly corresponding to the usual ISR, FSR, and MPI model elements, by choosing to use only one of the three VAR3 variations.

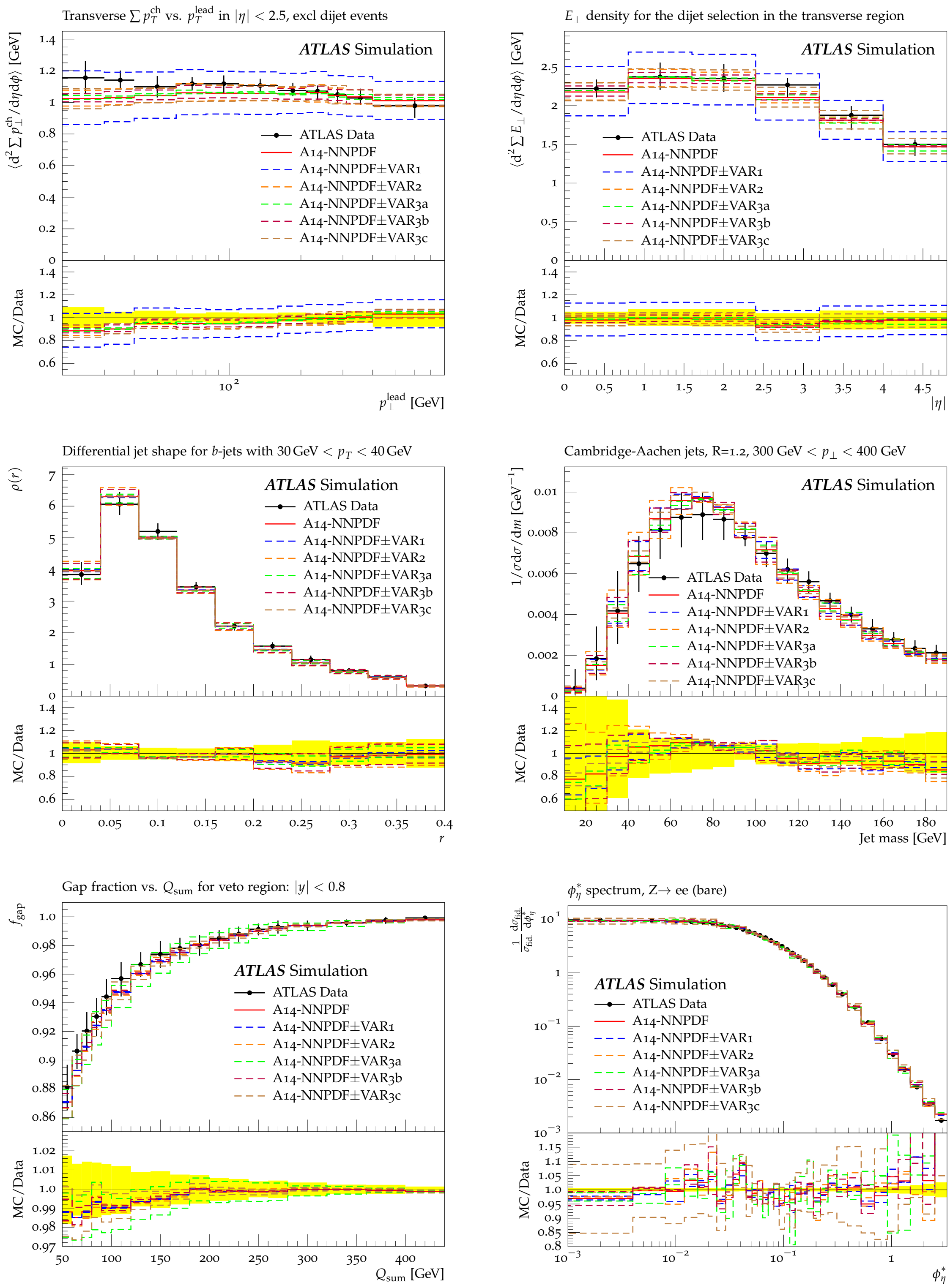

Figure 7: Demonstrations of the five pairs of eigentune variations. The top row illustrates distributions best covered by the VAR1 "MPI" variations, the middle row illustrates those best covered by the VAR2 "FSR" variations, and the bottom row shows two observables covered by VAR3a–c, affecting different aspects of the ISR/FSR mix. The yellow shaded areas represent data uncertainty.

4 Conclusions

In this note we have presented new tunes of the Pythia 8 event generator, suitable for use in high p_T processes and using four different PDFs. These tunes simultaneously optimised MPI and parton shower (ISR,FSR) parameters since these model features affect data observables in combination.

The new "A14" tunes lead to better description of UE data, $t\bar{t}$ gap fractions, and 3-to-2 jet ratios compared to the currently used AU2 tune, with very similar behaviours for all four PDFs. Five pairs of parameter variations on the A14-NNPDF tune have been obtained based on the results of the eigentune method, reduced to a minimal covering set. Depending on analysis details it may be possible to reduce this further to the usual 3 pairs of variations roughly corresponding to ISR, FSR, and MPI modelling.

The utility of these tunes for ATLAS sample production is intended to be mainly limited to situations where next-to-leading order (NLO) or multi-leg simulations are unavailable or are impractical – where they can be used, these simulations with higher-order matrix elements are preferable. However, this A14 tuning reveals that a good description of the kinematics of single-extra-emission matrix element modelling can be obtained with standalone Pythia 8 across a wide range of Standard Model process types, and further tunes for use with matched higher-order matrix elements and parton showers will incorporate the developments described here.

References

[1] T. Sjostrand, S. Mrenna, and P. Skands, Comput. Phys. Commun. **178** (2008) 852–867, arXiv:0710.3820 [hep-ph].

[2] The ATLAS Collaboration,, 2012. https://cds.cern.ch/record/1474107. ATL-PHYS-PUB-2012-003.

[3] The ATLAS Collaboration,, 2013. https://cds.cern.ch/record/1629317. ATL-PHYS-PUB-2013-017.

[4] The ATLAS Collaboration, Phys.Rev. D **86** (2012) 072004, arXiv:1208.0563 [hep-ex].

[5] The ATLAS Collaboration, Eur. Phys. J. C **74** (2014) 2965, arXiv:1406.0392 [hep-ex].

[6] The ATLAS Collaboration, Phys.Rev. **D84** (2011) 054001, arXiv:1107.3311 [hep-ex].

[7] The ATLAS Collaboration, Phys.Rev. **D83** (2011) 052003, arXiv:1101.0070 [hep-ex].

[8] The ATLAS Collaboration, Eur.Phys.J.C **73** (2013) 2676, arXiv:1307.5749 [hep-ex].

[9] The ATLAS Collaboration, JHEP **1205** (2012) 128, arXiv:1203.4606 [hep-ex].

[10] The ATLAS Collaboration, Phys.Rev.Lett. **106** (2011) 172002, arXiv:1102.2696 [hep-ex].

[11] The ATLAS Collaboration, Eur.Phys.J. C **72** (2012) 2043, arXiv:1203.5015 [hep-ex].

[12] The ATLAS Collaboration, Eur.Phys.J. **C71** (2011) 1763, arXiv:1107.2092 [hep-ex].

[13] The ATLAS Collaboration, Phys.Lett.B **705** (2011) 415–434, arXiv:1107.2381 [hep-ex].

[14] The ATLAS Collaboration, arXiv:1406.3660 [hep-ex].

[15] A. Buckley, J. Butterworth, L. Lonnblad, H. Hoeth, J. Monk, et al., arXiv:1003.0694 [hep-ph].

[16] A. Buckley, H. Hoeth, H. Lacker, H. Schulz, and J. E. von Seggern, arXiv:0907.2973 [hep-ph].

[17] J. Butterworth, G. Dissertori, S. Dittmaier, D. de Florian, N. Glover, et al., arXiv:1405.1067 [hep-ph].

[18] The ATLAS Collaboration,, 2011. http://cdsweb.cern.ch/record/1345343. ATL-PHYS-PUB-2011-008.

[19] The ATLAS Collaboration,, 2010. http://cdsweb.cern.ch/record/1363300. ATL-PHYS-PUB-2011-009.

[20] The ATLAS Collaboration,, 2011. http://cdsweb.cern.ch/record/1400677. ATL-PHYS-PUB-2011-014.

[21] The ATLAS Collaboration, arXiv:1409.3433 [hep-ex].

[22] P. Skands, S. Carrazza, and J. Rojo, European Physical Journal C **74** (2014) 3024, arXiv:1404.5630 [hep-ph].

[23] J. Pumplin et al., JHEP **07** (2002) 012, arXiv:hep-ph/0201195.

[24] G. Watt and R. Thorne, arXiv:1205.4024 [hep-ph].

[25] S. Carrazza, S. Forte, and J. Rojo, arXiv:1311.5887 [hep-ph].

[26] A. M. Cooper-Sarkar, PoS **DIS2014** (2014) 032.

[27] The ATLAS Collaboration, Phys.Lett. **B720** (2013) 32–51, arXiv:1211.6899 [hep-ex].

[28] The ATLAS Collaboration, JHEP11(2012)033 (2012), arXiv:1208.6256 [hep-ex].

[29] The CMS Collaboration, JHEP **1111** (2011) 148, arXiv:1110.0211 [hep-ex].